Pseudorange Rigidity and Solvability of Cooperative GNSS Positioning

Colin Cros, Pierre-Olivier Amblard, Christophe Prieur, Jean-François Da Rocha

Pseudorange Rigidity and Solvability of Cooperative GNSS Positioning

Colin Cros, Pierre-Olivier Amblard, Christophe Prieur and Jean-François Da Rocha

***Abstract*— Global Navigation Satellite Systems (GNSS) are a widely used technology for positioning and navigation. GNSS positioning relies on pseudorange measurements from satellites to receivers. A pseudorange is the apparent distance between two agents deduced from the time-of-flight of a signal sent from one agent to the other. Because of the lack of synchronization between the agents' clocks, it is a biased version of their distance. This paper introduces a new rigidity theory adapted to pseudorange measurements. The peculiarity of pseudoranges is that they are asymmetrical measurements. Therefore, unlike other usual rigidities, the graphs of pseudorange frameworks are directed. In this paper, pseudorange rigidity is proved to be a generic property of the underlying undirected graph of constraints. The main result is a characterization of rigid pseudorange graphs as combinations of rigid distance graphs and connected graphs. This new theory is adapted for GNSS. It provides new insights into the minimum number of satellites needed to locate a receiver, and is applied to the localization of GNSS cooperative networks of receivers. The interests of asymmetrical constraints in the context of formation control are also discussed.**

I. Introduction

Global Navigation Satellite Systems (GNSS) provide an effective and low-cost solution for localization. They rely on constellations of satellites, equipped with highly accurate atomic clocks. In these systems, the satellites broadcast signals that contain information about the precise location of the emitting satellite as well as the time of emission of the signal transmitted [17]. These signals are received by GNSS receivers on the ground. The receivers measure the time of reception and deduce the times-of-flight of the signals. These times are converted into distances by multiplying by the signal's celerity. As the receivers are generally not synchronized with the satellites, the distance obtained is a biased version of the distance between the satellite and the receiver. It is called a *pseudorange*. The bias comes from the delay between the satellite's clock and the receiver's clock that is also multiplied by the signal's celerity. This bias is the same for every satellite within a GNSS constellation and must be estimated. Indeed, a delay of 10ns would produce a range error of about 3m. By receiving signals from multiple satellites, a receiver can determine its position on the Earth's surface by solving the nonlinear system of equations induced by the pseudoranges. Therefore, GNSS positioning is a multilateration problem, similar to other systems that were used before it, such as the *Long Range Navigation* (LORAN) systems [9].

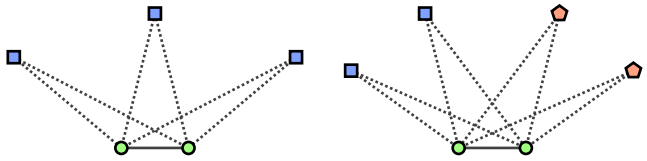

(a) Monoconstellation. (b) Bi-constellation

Fig. 1: Graph of measurements of cooperative networks. Each network is composed of two GNSS receivers represented by circles. One constellation of satellites is represented by squares and another by pentagons. The dotted lines represent pseudorange measurements, and the solid lines inter-receiver distance measurements.

The minimum number of pseudorange measurements required to locate a receiver is $3+C$ where C is the number of GNSS constellations used. The usual justification is that there are $3+C$ unknowns in the system: 3 for the receiver position, plus 1 per GNSS constellation clock bias. Each pseudorange equation is used to solve for one unknown, and therefore the localization problem is solvable with $3+C$ pseudoranges. The recent development of network systems raises the question of their cooperative positioning. When a node is unable to use GNSS (completely or partially), it can cooperate with the other nodes in the network to estimate its position, e.g., by measuring distances with its neighbors and performing trilateration. Collaborative positioning has been proved to be an efficient solution to improve the precision [19] and to extend the availability [6] of the GNSS. However, the localizability of a network of receivers from a set of given measurements has never been answered and, in general, the minimal number of pseudorange measurements required for locating a network is unknown. For example, consider a pair of receivers measuring pseudoranges from only $2+C$ satellites from C different GNSS constellations. They cannot estimate their positions as it would require one additional measurement. Assume they also measure the distance between them, as illustrated in Figure 1.

C. Cros, P.O. Amblard and C. Prieur are with the CNRS, Univ. Grenoble Alpes, GIPSA-lab, F-38000 Grenoble, France. colin.cros@gipsa-lab.fr, christophe.prieur@gipsa-lab.fr, pierre-olivier.amblard@cnrs.fr.
C. Cros and J.F. Da Rocha are with Telespazio FRANCE, F-31100 Toulouse, France. jeanfrancois.darocha@telespazio.com.

With this additional measurement, can they estimate their positions? The aim of this paper is to answer this question for a general class of cooperating networks. The solvability of such localization problems is intrinsically linked to the notion of rigidity; their connections have been detailed when considering only distance measurements in e.g., [3].

Rigidity is the capacity of a structure to maintain its shape by solely maintaining some constraints between pairs of nodes (called agents in the sequel). Rigidity was first introduced with distance constraints to study the stability of bar-and-joint structures, see e.g., [15] for an introduction. Since then, it has been adapted to other forms of interactions between the agents, e.g., bearing rigidity [30] and angle rigidity [7] have been derived for agents equipped with cameras providing the angles or the bearings between the agents. Recently, Joint Position-Clock (JPC) rigidity [29] has been introduced to treat symmetrical time-of-flight measurements. Unfortunately, in GNSS, the signals are sent only from satellites to receivers, which results in asymmetrical measurements. Most of the rigidities introduced in the literature are based on symmetrical measurements and symmetrical constraints. Consequently, the frameworks are described by undirected graphs of constraints. Pseudoranges are by nature asymmetrical, and therefore they cannot be treated with the existing rigidity theories.

In this paper, we focus on sensor networks performing pseudorange measurements and distance measurements. We answer the question of the localizability of the network given the set of measurements, i.e., we answer the following question. Is the positions of the agents identifiable given the measurements? To answer this question, we introduce and characterize a new form of asymmetrical rigidity adapted to the pseudorange context. The main contributions are the following:

1) Pseudorange rigidity is introduced. The main difference with the usual rigidities is that the graphs of pseudorange frameworks are directed to account for the asymmetry of the measurements. We prove that pseudorange rigidity is a generic property of the underlying undirected graph. Furthermore, we prove that the rank of the pseudorange rigidity matrix can be expressed by separating the spatial variables from the clock parameters. The consequence is that a pseudorange graph is rigid if and only if it is the combination of a distance rigid graph and a connected graph.
2) Pseudorange rigidity is extended to define the rigidity of GNSS networks. GNSS rigidity brings a new justification to the common wisdom about the minimum number of satellites required to locate a single receiver. Furthermore, it applies to cooperative networks of GNSS receivers. It helps to identify the connections required to locate a network and to design localization algorithms.
3) The interests of pseudorange rigidity for formation control are presented. To preserve the 2D formation of a group of agents, the pseudorange point of view allows to reduce by up to 25% the number of measurements, with respect to a classical two-way ranging method. For 3D formations, this number is reduced by up to 33%.
4) New algebraic concepts are exposed to isolate spatial variables from the other variables in rigidity matrices. The technique employed in this paper may be reused for other types of rigidity, e.g., JPC rigidity [29].

The rest of this paper is organized as follows. Section II introduces the notion of pseudorange and provides some background on rigidity. Pseudorange rigidity is introduced in Section III. The rigidity of pseudorange graphs is characterized in Section IV. Section V adapts these new results to the GNSS context and Section VI discusses the applications of pseudorange rigidity for formation control. Finally, Section VII gives some perspectives.

Notation. In the sequel, matrices are denoted in uppercase boldface variables e.g., $\boldsymbol{M} \in \mathbb{R}^{n\times m}$, and the Euclidean norm of a vector is denoted as $\|x\|$. The dimension of the space in which the agents live is denoted as d, and it is assumed set. In practice $d = 3$, but the results presented here are valid for any $d \geq 2$. A simple graph with a vertex set V and an edge set E is denoted as $G = (V, E)$. Undirected simple graphs are named with Latin letters, e.g., G, while directed simple graphs are named with Greek letters, e.g., Γ. A directed edge is called an arc. For a simple directed graph $\Gamma = (V, E)$, $\tilde{\Gamma} = (V, \tilde{E})$ denotes the undirected multigraph induced by Γ where $\tilde{E}$ denotes the multiset of the edges. An edge can appear 0 times once or twice in the $\tilde{E}$. For a general background on graph definitions and properties (incidence matrix, connectivity, cycles, etc.), we refer to [5]. The cardinality of a set A is denoted as $|A|$.

II. Preliminaries

A. Pseudorange measurements

In the sequel, "agent" is a generic term referring to satellites and receivers. In the context of GNSS, a pseudorange is an indirect measurement of a distance between two agents based on the time-of-flight of a signal. As the time of emission and the time of reception of the signal are measured by two different and potentially unsynchronized clocks, it is a biased version of the distance. The time t^i given by the clock of the ith agent is modeled as:

$$t^i = t + \tau_i, \tag{1}$$

where t is some virtual absolute time and τ_i is the bias with respect to that time. The position of the ith agent is denoted as $x_i \in \mathbb{R}^d$. Its clock bias is taken premultiplied by the signal's celerity c to be homogeneous to a length, and it is denoted as $\beta_i \triangleq c\tau_i$. The pseudorange from an agent u to another v is:

$$\rho_{uv} \triangleq c\left(t^v_{r(uv)} - t^u_{e(uv)}\right) = \|x_u - x_v\| + \beta_v - \beta_u \tag{2}$$

where $t_{e(uv)}$ and $t_{r(uv)}$ denote respectively the time of emission and the time of reception of a signal sent from u to v. Note that the pseudorange equals the distance if and only if $\beta_u = \beta_v$, i.e., if the agents' clocks are synchronized.

B. Generalities on rigidity

Consider a network composed of n agents in $\mathbb{R}^d$. The ith agent is characterized by a vector p_i. Usually p_i is the position $x_i \in \mathbb{R}^d$ of the agent, but p_i can contain other

parameters such as clock parameters. The **configuration** of the network is the vector $p = \begin{bmatrix} p_1^\intercal & \dots & p_n^\intercal \end{bmatrix}^\intercal$. The interactions between the agents are represented in a graph $G = (V, E)$. The edges in E represent constraints between the agents in V, e.g., distance constraints or bearing constraints. The number of constraints is $m = |E|$. The pair (G, p) is called a **framework**. The evaluation of the constraints is the vector $F_X(G,p) = \begin{pmatrix} \dots & f_{X,uv}(p)^\intercal & \dots \end{pmatrix}^\intercal \in \mathbb{R}^{mk_X}$, where in this definition X denotes the type of rigidity, $f_{X,uv}(p) \in \mathbb{R}^{k_X}$ is the evaluation of the constraint induced by the edge $uv \in E$, and the edges are assumed to be ordered.

Two frameworks (G, p) and (G, p') are said to be **equivalent** if $F_X(G,p) = F_X(G,p')$. They are said to be **congruent** if $F_X(K,p) = F_X(K,p')$, where K is the complete graph whose edge set is $E_K = \{uv \in V^2, u < v\}$.

A framework (G, p) is **rigid** if there exists $\epsilon > 0$ such that for all p' satisfying $\|p - p'\| < \epsilon$, (G, p) and (G, p') equivalent implies (G, p) and (G, p') congruent. A non-rigid framework is called **flexible**. A framework (G, p) is **globally rigid** if for all p', (G, p) and (G, p') equivalent implies (G, p) and (G, p') congruent.

The **rigidity matrix** [15] of a framework is defined as the Jacobian of the evaluation function:

$$\boldsymbol{R}_X(G,p) \triangleq \frac{\partial F_X(G,p)}{\partial p}. \tag{3}$$

A **velocity vector** [15] q is a variation of p. If $\boldsymbol{R}_X(G,p)q = 0$, q is said to be **admissible** for the framework. A velocity vector admissible for all frameworks is called **trivial**. A framework (G, p) is **infinitesimally rigid** if all its admissible velocity vectors are trivial.

C. Different rigidities

This section provides a summary of different forms of rigidity. It does not intend to be exhaustive but focuses on the rigidities related with pseudorange rigidity introduced in the next section.

1) Distance rigidity: Distance rigidity is the original and most studied rigidity. An agent is represented by its spatial coordinates $p_i = x_i \in \mathbb{R}^d$ and the edges of G constrain the distances between pairs of agents. The constraint induced by an edge uv is $f_{D,uv}(p) \triangleq \|x_u - x_v\| = \delta_{uv}$ where δ_{uv} is a given distance. The trivial motions correspond to translations and rotations of the framework.

2) Distance rigidity in elliptical and hyperbolic space: Distance rigidity has been extended to non-Euclidean spaces, see e.g., [25], [28]. An interesting case for our study is the Minkowski hyperbolic space. In this case, the agents are parameterized by $p_i = \begin{pmatrix} x_i^\intercal & \gamma_i \end{pmatrix}^\intercal \in \mathbb{R}^{d+1}$, where γ_i is a scalar. The constraint induced by an edge is $f_{M,uv}(p) \triangleq \|x_u - x_v\|^2 - (\gamma_u - \gamma_v)^2 = \delta_{uv}$ where δ_{uv} is a given "distance" (that may be negative). Unlike a pseudorange, the Minkowski distance $f_{M,uv}(p)$ is symmetrical in u and v.

3) Bearing rigidity: Bearing rigidity focuses on preserving the shape of a framework by constraining the bearings between the agents, see e.g., [31] for an overview. The ith agent is also represented by its spatial coordinates $p_i = x_i \in \mathbb{R}^d$. The constraint induced by an edge uv of the graph is $f_{B,uv}(p) \triangleq \frac{x_u - x_v}{\|x_u - x_v\|} = \boldsymbol{\alpha}_{uv} \in \mathbb{R}^d$ where $\boldsymbol{\alpha}_{uv}$ is a given bearing. The trivial motions correspond to translations and stretching of the framework.

4) Clock rigidity: Clock rigidity was recently introduced in [29]. It focuses on preserving the synchronization between the clocks of the agents. The clock model considered in clock rigidity has two parameters. The time t^i of the ith agent's clock is modeled as:

$$t^i = w_i t + \tau_i, \qquad \Leftrightarrow \qquad t = \alpha_i t^i + \lambda_i, \tag{4}$$

where w_i and α_i are clock skews, and τ_i and λ_i are clock biases. The ith agent's clock is parameterized by $p_i = (\alpha_i, \lambda_i) \in \mathbb{R}^2$. The authors assumed that times-of-flight are always measured in both directions [29, Assumption 1]. Under this assumption, each pair of measurements imposes:

$$\|x_u - x_v\| = c(\alpha_v t^v_{r(uv)} + \lambda_v - \alpha_u t^u_{e(uv)} - \lambda_u), \tag{5a}$$
$$\|x_u - x_v\| = c(\alpha_u t^u_{r(vu)} + \lambda_u - \alpha_v t^v_{e(vu)} - \lambda_v). \tag{5b}$$

Therefore, an edge uv of G induces the following constraint on the clock parameters: $f_{C,uv}(p) \triangleq \alpha_u \bar{T}^u + \lambda_u - \alpha_v \bar{T}^v - \lambda_v = 0$ where $\bar{T}^u$ and $\bar{T}^v$ are constant. The authors proved that clock rigidity is strongly connected with bearing rigidity in 2D [29].

5) Joint Position-Clock rigidity: JPC rigidity was also introduced in [29] to preserve both the distances and the clock synchronizations between the agents. In this case, $p_i = \begin{pmatrix} x_i^\intercal & \alpha_i & \lambda_i \end{pmatrix}^\intercal \in \mathbb{R}^{d+2}$ is the combination of the spatial coordinates and the clock parameters of the agents. The edges of G constrain the two times-of-flight between the agents (in both directions). An edge $uv \in G$ constrains the two constraints (5). To study JPC rigidity, the authors of [29] used the bi-directional assumption to separate the distance constraint from the clock constraint.

6) Coordinated rigidity: Coordinated rigidity was introduced in [20], [27]. It is an extension of distance rigidity that allows a new type of movements. The edges are split into groups and the edges among a group can expand simultaneously. Formally, the graph is enriched with a coloration of its edges $c = (E_0, \dots, E_k)$, and the configuration is enriched with a vector $r \in \mathbb{R}^k$ associating to each color a bias. Two frameworks (G, c, p, r) and (G, c, p', r') are said to be equivalent if:

$$\begin{aligned} \|p_u - p_v\| &= \|p'_u - p'_v\| && \forall uv \in E_0, \\ \|p_u - p_v\| + r_l &= \|p'_u - p'_v\| + r'_l && \forall uv \in E_l,\ 1 \le l \le k. \end{aligned}$$

This context fits for GNSS: each color corresponds to a pair receiver-constellation and each bias to the offset of the receiver's clocks on the constellation time. The pseudorange point of view is however more general, e.g., it can be applied if the receivers cooperate by pseudorange measurements.

D. About the lack of asymmetrical rigidity

All the constraints presented Section II-C are symmetrical: there is no difference between constraining the pair (u, v) or the pair (v, u). For clock rigidity and JPC rigidity, even if the measurements are not symmetrical, the symmetry comes from the fact that the times-of-flight are measured in both directions. The specificity of our study lies in the asymmetry

of the pseudoranges. In the GNSS context, we cannot assume that the pseudoranges are measured in both directions as they are taken only from satellites to receivers. This motivates the need to study pseudorange rigidity as a new concept. The important difference with the literature is that pseudorange graphs are directed to account for the asymmetry of the measurements. JPC rigidity can also be considered in an asymmetrical context. In Section VI, we discuss this extension and the main difference with pseudorange rigidity.

III. Pseudorange rigidity

A. Pseudorange frameworks

Consider a network of n agents, the ith agent is parameterized by $p_i = \begin{pmatrix} x_i^\intercal & \beta_i \end{pmatrix}^\intercal \in \mathbb{R}^{d+1}$ where x_i is its position and β_i its clock bias. Consider also a directed graph $\Gamma = (V, E)$ representing the pseudorange measurements between the agents. The set E is a set of arcs (directed edges). To maintain generality, no restriction on the topology of the graph is imposed. For a pair of vertices $(u, v) \in V^2$, E can contain the arc uv, the arc vu, both arcs or none of them. The pseudorange configuration is the vector $p = \begin{pmatrix} x_1^\intercal & \dots & x_n^\intercal & \beta_1 & \dots & \beta_n \end{pmatrix}^\intercal \in \mathbb{R}^{n(d+1)}$ and the pseudorange framework is the pair (Γ, p). Note that the spatial parameters have been grouped for convenience. An arc uv imposes the constraint:

$$f_{P,uv}(p) \triangleq \|x_u - x_v\| + \beta_v - \beta_u = \rho_{uv}, \tag{6}$$

where ρ_{uv} is a given pseudorange. The definition of congruence, equivalence, and rigidity of pseudorange frameworks are the same as introduced in Section II-B. However, K is now the complete directed graph whose arc set is $E_K = \{uv \in V^2, u \neq v\}$.

The complexity of pseudorange rigidity comes from the asymmetry of Γ. Without this asymmetry, the problem would be of no interest. Indeed, two opposite pseudoranges ρ_{uv} and ρ_{vu} constrain both the distance and the bias difference between the agents:

$$\|x_u - x_v\| = \frac{\rho_{uv} + \rho_{vu}}{2}, \qquad \beta_u - \beta_v = \frac{\rho_{vu} - \rho_{uv}}{2}. \tag{7}$$

In that case, the spatial constraints and the bias constraints can be separated. To rigidify the biases, the graph must be connected, and to rigidify the positions, the graph must be distance rigid. As distance rigid graphs are connected, pseudorange rigidity and distance rigidity are equivalent for symmetrical pseudorange graphs. The study of pseudorange rigidity is however far less trivial when Γ is not symmetrical.

The decoupling between the spatial and the bias constraints can also be performed if Γ has a spanning tree of symmetrical arcs. In that case, all the bias differences are also set, and pseudorange constraints become distance constraints. Hence, if Γ has a spanning tree of symmetrical arcs, pseudorange rigidity and distance rigidity are also equivalent. Our main result in Section IV states that in fact, the spanning tree does not need to be formed of symmetrical arcs: a pseudorange graph is rigid if a distance rigid graph can be extracted while the remaining arcs form a connected graph. This result is based on the characterization of pseudorange infinitesimal rigidity, and therefore on the characterization of the rank of the pseudorange rigidity matrix.

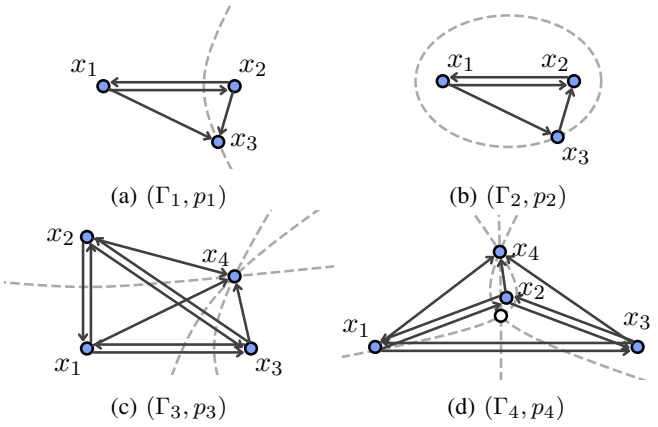

Fig. 2: Examples of 2-dimensional pseudorange frameworks. The positions of the agents are represented by blue circles, the pseudorange constraints by arrows. The dashed curves are construction lines for the position of the last agent and the white circle in Fig. 2d is another possible position for the 4th agent. The bias axis is not represented.

Section III-B proposes four examples of pseudorange frameworks to underline the importance of the orientation of the arcs, and then Section III-C introduces pseudorange generic rigidity. The main results, Theorem 1 and its Corollaries 1-2, are stated in Section IV.

B. Examples of pseudorange frameworks

Figure 2 presents four 2-dimensional pseudorange frameworks. Each agent has 2 spatial coordinates plus 1 clock bias. This paragraph investigates their rigidity.

First, consider the framework in Figure 2a. This framework has 4 arcs corresponding to the pseudoranges from 1 to 2, from 2 to 1, from 1 to 3 and from 2 to 3. They constrain the following equations:

$$\|x_1 - x_2\| + \beta_2 - \beta_1 = \rho_{1,2}, \tag{8a}$$
$$\|x_1 - x_2\| + \beta_1 - \beta_2 = \rho_{2,1}, \tag{8b}$$
$$\|x_1 - x_3\| + \beta_3 - \beta_1 = \rho_{1,3}, \tag{8c}$$
$$\|x_2 - x_3\| + \beta_3 - \beta_2 = \rho_{2,3}. \tag{8d}$$

Since both pseudoranges between agents 1 and 2 are constrained, their distance and bias difference are set using (7). Moreover, since the pseudoranges $\rho_{1,3}$ and $\rho_{2,3}$ are also constrained, subtracting (8d) from (8c) gives:

$$\|x_1 - x_3\| - \|x_2 - x_3\| = \rho_{1,3} - \rho_{2,3} + \beta_1 - \beta_2 = \text{cst}. \tag{9}$$

Therefore, the position of agent 3 lies on a branch of hyperbola whose foci are x_1 and x_2. This branch is represented by the dashed line in the figure. The bias β_3 is obtained by reinjecting the distance into either (8c) or (8d) and is not constant along this curve: it decreases as the distance $\|x_1 - x_3\|$ increases. Moving agent 3 along this 3-dimensional curve of positions

creates a non-congruent but equivalent configuration, therefore, this framework is flexible.

The second framework in Figure 2b is very similar. The only difference lies in the direction of the arc between 2 and 3. In Figure 2a, $\rho_{2,3}$ was constrained whereas it is now $\rho_{3,2}$. This transforms (8d) to:

$$\|x_2 - x_3\| + \beta_2 - \beta_3 = \rho_{3,2}. \tag{10}$$

Moreover, summing (8c) and (10) gives:

$$\|x_1 - x_3\| + \|x_2 - x_3\| = \rho_{1,3} + \rho_{3,2} + \beta_1 - \beta_2 = \text{cst}. \tag{11}$$

Consequently, x_3 lies on an ellipse, also represented by a dashed line in the figure. Similarly, moving agent 3 on this curve of positions creates a non-congruent but equivalent configuration and this framework is flexible. These first two examples underline how important the orientations of the arcs are: flipping an arc changes the possible deformations of the framework.

The third and fourth frameworks in Figures 2c and 2d have the same graph which is more complex. The first three agents are fully connected, therefore, all the distances and bias differences between them are constrained: their relative positions and biases are set. The 4th agent is connected to each of them by one unique arc. Each pair of arcs constrains the position x_4 to lie on a branch of hyperbola as in the first example. These curves are also represented by dashed lines. For the third framework, they intersect once at x_4, this is the only suitable position for the 4th agent. There are no equivalent but non-congruent frameworks, therefore, (Γ_3, p_3) is globally rigid. For the fourth framework, they intersect twice: at x_4 of course and at a second point represented by a white circle. Those two points are suitable positions for agent 4: placing it in one of these loci (with the corresponding bias) satisfies all the constraints. However, agent 4 cannot *move* so the framework is rigid but not globally rigid. At these two loci, the associated biases are different since, for example, the distances to x_2 are different.

C. Pseudorange generic rigidity

This section introduces pseudorange generic rigidity and its link with pseudorange infinitesimal rigidity. In particular, the properties of the pseudorange rigidity matrix are discussed.

Definition 1. *A pseudorange configuration p is said to be* generic *if the nd spatial coordinates of the agents are not a root of any non-trivial polynomial with integer coefficients. In this case, the framework (Γ, p) is also said to be generic.*

Genericity ensures, for example, that no three agents are aligned or that no four agents are on a plane. In practice, the agents are never perfectly aligned and the configuration is generic. Formally, the set of non-generic configurations is defined as the roots of the polynomials with integer coefficients. Therefore, it is countable and has a 0 measure. Consequently, *almost* every configuration is generic. Note that this property considers the positions of the agents but not their clock offsets.

As for distance frameworks, the rigidity of generic pseudorange frameworks is equivalent to their infinitesimal rigidity, as stated in the following lemmas.

Lemma 1. *If a pseudorange framework (Γ, p) is infinitesimally rigid, then it is rigid.*

Lemma 2. *Let (Γ, p) be a generic pseudorange framework. (Γ, p) is rigid if and only if it is infinitesimally rigid.*

The proofs of Lemmas 1 and 2 are adaptions of proofs on distance rigidity of usual distance frameworks and will not be detailed. They can be found e.g., in [2] or [10].

Consequently, to study the generic rigidity of pseudorange frameworks, we focus on their rigidity matrices. To match the usual form of rigidity matrix, we define the pseudorange rigidity matrix of the framework as follows:

$$\boldsymbol{R}_P(\Gamma, p) \triangleq \boldsymbol{D}(\Gamma, p) \frac{\partial F_P(\Gamma, p)}{\partial p} \in \mathbb{R}^{m \times n(d+1)}, \tag{12}$$

where $\boldsymbol{D}(\Gamma, p) = \text{diag}\left(\{\|x_u - x_v\|, uv \in E\}\right)$ is the diagonal matrix whose ith entry is the distance between the points connected by the ith arc. With this definition, the pseudorange rigidity matrix has the following structure:

$$\boldsymbol{R}_P(\Gamma, p) = \begin{bmatrix} \boldsymbol{R}_D(\Gamma, p) & \boldsymbol{R}_S(\Gamma, p) \end{bmatrix}, \tag{13}$$

where $\boldsymbol{R}_D(\Gamma, p) \in \mathbb{R}^{m \times nd}$ is the distance rigidity matrix of the framework (where Γ is viewed as an undirected multigraph), and $\boldsymbol{R}_S(\Gamma, p) \in \mathbb{R}^{m \times n}$ is a rigidity matrix associated with the synchronizations of the clocks. It corresponds to the clock offset variables and is defined as:

$$\boldsymbol{R}_S(\Gamma, p) = \boldsymbol{D}(\Gamma, p) \boldsymbol{B}(\Gamma)^\intercal, \tag{14}$$

where $\boldsymbol{B}(\Gamma)$ denotes of the incidence matrix of the graph Γ, see e.g., [5, p. 54]. For example, the rigidity matrix of the pseudorange framework in Figure 2a is given in (15) at the top of the next page.

From the decomposition (13), the rank of the pseudorange rigidity matrix is lower than the sum of the ranks of each block. The rank of the distance rigidity matrix is bounded by a quantity $S_D(n, d)$ [2] defined as:

$$S_D(n, d) \triangleq \begin{cases} nd - \binom{d+1}{2} & \text{if } n \geq d+1, \\ \binom{n}{2} & \text{if } n \leq d. \end{cases}. \tag{16}$$

Moreover, the maximal rank of an incidence matrix between n agents is $n-1$: the vector filled with ones is always in the cokernel of the incidence matrix. As a result, the rank of the rigidity matrix is bounded by a quantity $S_P(n, d)$ that depends on both the number of agents n and the dimension d:

$$\text{rank}\, \boldsymbol{R}_P(\Gamma, p) \leq S_P(n, d) \triangleq S_D(n, d) + n - 1. \tag{17}$$

The interpretation of (17) is that the trivial velocity vectors are composed of the d spatial translations, the $d(d-1)/2$ spatial rotations and the bias translation.

Definition 2. *A pseudorange framework (Γ, p) is said to be* infinitesimally rigid *if* $\text{rank}\, \boldsymbol{R}_P(\Gamma, p) = S_P(n, d)$.

The next section proves that, generically, infinitesimal rigidity is a property of the graph.

$$R_P(\Gamma,p)=\left[\begin{array}{ccc|ccc} x_1^\intercal-x_2^\intercal & x_2^\intercal-x_1^\intercal & 0^\intercal & -\|x_1-x_2\| & \|x_1-x_2\| & 0 \\ x_1^\intercal-x_2^\intercal & x_2^\intercal-x_1^\intercal & 0^\intercal & \|x_1-x_2\| & -\|x_1-x_2\| & 0 \\ x_1^\intercal-x_3^\intercal & 0^\intercal & x_3^\intercal-x_1^\intercal & -\|x_1-x_3\| & 0 & \|x_1-x_3\| \\ 0^\intercal & x_2^\intercal-x_3^\intercal & x_3^\intercal-x_2^\intercal & 0 & -\|x_2-x_3\| & \|x_2-x_3\| \end{array}\right] \tag{15}$$

IV. Characterization of generic pseudorange rigidity

In this section, we provide a complete characterization of the rigidity of generic pseudorange frameworks in terms of distance rigidity. We prove that pseudorange rigidity is a generic property of the underlying undirected graphs of the frameworks. We explicit the rank of the rigidity matrix according to possible *decompositions* of the graph. Our approach is similar to the one used for distance frameworks in e.g., [12]. The rank is considered as the order of a highest order non-vanishing minor of the matrix.

For distance frameworks the minors of the rigidity matrix $\boldsymbol{R}_D(G,p)$ are polynomials with integer coefficients in the nd coordinates of the agents. By definition of a generic configuration, a minor vanishes for a generic configuration only if it is the null function (in this case, it vanishes for every configuration). For pseudorange rigidity matrices, the minors are also functions of the nd coordinates of the agents. However, contrary to the minors of distance rigidity matrices, these minor functions are not polynomials. They belong to a larger space of functions we call $\mathbb{L}$. Recall that (15) gives an example of a pseudorange rigidity matrix.

We define the space $\mathbb{L}$ as follows. For any set of edges $E\subseteq\{uv \mid 1\leq u<v\leq n\}$, we define the space $\mathbb{L}(E)$ as:

$$\mathbb{L}(E)=\left\{\sum_{F\in\boldsymbol{\mathcal{P}}(E)} P_F\prod_{uv\in F} D_{u,v} \mid P_F\in\mathbb{K}\right\} \tag{18}$$

where $\mathbb{K}=\mathbb{Q}\left(X_1^{(1)},\dots,X_n^{(d)}\right)$ is the field of rational functions with integer coefficients in nd variables, $\boldsymbol{\mathcal{P}}(E)$ denotes the power set of E, and $D_{u,v}$ is the distance function in nd variables:

$$D_{u,v}:(x_1^{(1)},\dots,x_n^{(d)})\mapsto\sqrt{\sum_{i=1}^{d}\left(x_u^{(i)}-x_v^{(i)}\right)^2}. \tag{19}$$

Then, the minors of the pseudorange rigidity matrix of a framework (Γ,p) whose underlying undirected graph is $\tilde{\Gamma}=(V,\tilde{E})$ belong to the space $\mathbb{L}=\mathbb{L}(\tilde{E})$.

The definitions of $\mathbb{L}(E)$ and $\mathbb{K}$ may seem overly complex. They have both been chosen to provide a field structure to $\mathbb{L}(E)$ as stated in the following lemma.

Lemma 3. *Let $E\subseteq\{uv \mid 1\leq u<v\leq n\}$ be a set of edges and $m=|E|$. Then, $\mathbb{L}(E)/\mathbb{K}$ is a field extension of degree 2^m. Furthermore, the family $\left\{\prod_{uv\in F} D_{u,v} \mid F\in\boldsymbol{\mathcal{P}}(E)\right\}$ is a basis of $\mathbb{L}(E)$ viewed as a $\mathbb{K}$-vector space. We call this basis the* natural basis *of $\mathbb{L}(E)$.*

Lemma 3 involves several elements from field theory. They will not be discussed here, nonetheless, these concepts can be found e.g., in [24] and the proof of Lemma 3 is provided in Appendix I for the sake of completeness. Solely the implications of this lemma are explained here. The first important point is that $\mathbb{L}$ is a field. Therefore, every nonzero element has a multiplicative inverse. Second, $\mathbb{L}$ is a $\mathbb{K}$-vector space of dimension 2^m and one natural basis is known. For example, if $E=\{ab,bc,ac\}$, the natural basis of $\mathbb{L}$ has 8 elements: the constant function equals to 1, the three distance functions $D_{a,b}$, $D_{b,c}$ and $D_{a,c}$, the three products of two distance functions $D_{a,b}D_{b,c}$, $D_{b,c}D_{a,c}$ and $D_{a,c}D_{a,b}$, and the product of the three distance functions $D_{a,b}D_{b,c}D_{a,c}$. The last important consequence of Lemma 3 is that the polynomials P_F involved in (18) are unique as they are the coordinates on the natural basis.

By definition, the only polynomial with integer coefficents that vanishes at a generic point of $\mathbb{R}^{nd}$ is the zero polynomial. The structure of $\mathbb{L}$ allows to extend this property to the field $\mathbb{L}$ as explained in the following lemma.

Lemma 4. *Let $E\subseteq\{uv \mid 1\leq u<v\leq n\}$ be a set of edges and $f\in\mathbb{L}(E)$. If $\exists x\in\mathbb{R}^{nd}$ a generic vector such that $f(x)=0$, then $f=0$.*

Proof. Let x be a generic vector and $m=|E|$. For every $E'\subseteq E$, by Lemma 3, $\mathbb{L}(E')$ is a field and a $\mathbb{K}$-vector space of dimension $2^{|E'|}$ whose natural basis is composed of the products between the distance functions.

Let us prove the lemma by induction on the number of distance functions appearing in the expression of f. Let us prove that: $\forall k\in\{0,\dots,m\}$, if $f\in\mathbb{L}(E')$ with $|E'|=k$ and if $f(x)=0$, then $f=0$.

Base case: If $k=0$, f is a rational function with integer coefficients, i.e., $f=P/Q$ with P and Q two polynomials with integer coefficients. By definition, since x is generic and $P(x)=0$, P is the null function and therefore $f=0$.

Inductive step: Let E' have cardinality $k+1$ with $k\geq 0$, $f\in\mathbb{L}(E')$ with $f(x)=0$, and $uv\in E'$. Any function $h\in\mathbb{L}(E')$ can be uniquely decomposed, by separating the natural basis of $\mathbb{L}(E')$, as $h_1+D_{u,v}h_2$ with $h_1,h_2\in\mathbb{L}(E'\setminus\{uv\})$. Let $f=f_1+D_{u,v}f_2$ be this decomposition applied to f. Furthermore, let $\bar{f}=f_1-D_{u,v}f_2$ and $g=f\bar{f}=f_1^2-D_{u,v}^2f_2^2$. As $D_{u,v}^2$ is a polynomial, $g\in\mathbb{L}(E'\setminus\{uv\})$ where $E'\setminus\{uv\}$ has cardinality k. Since f vanishes at x, g also vanishes at x and by the induction hypothesis, $g=0$. Therefore, since $\mathbb{L}(E')$ is a field, either $f=0$ or $\bar{f}=0$. By definition, f and $\bar{f}$ have the same coordinates up to a sign in the natural basis, thus $f=0$. □

As the nd spatial coordinates of a generic framework form a generic point of $\mathbb{R}^{nd}$, Lemma 4 implies that the rank of the pseudorange rigidity matrix is a generic property of its graph Γ and of its underlying undirected graph $\tilde{\Gamma}$. We prove

in the sequel a stronger result: the rank can be expressed using *decompositions* of $\tilde{\Gamma}$.

Definition 3. *Let $\tilde{\Gamma} = (V, \tilde{E})$ be the underlying undirected graph of a directed graph $\Gamma = (V, E)$. Denote E_1 the set of edges that appear once in $\tilde{E}$ and E_2 the set of edges that appear twice in $\tilde{E}$. Two simple graphs $G_D = (V, E_D)$ and $G_S = (V, E_S)$ are said to form a* decomposition *of the multigraph $\tilde{\Gamma} = (V, \tilde{E})$ if:*

1) $E_D \cup E_S = E_1 \cup E_2$.
2) $E_D \cap E_S = E_2$.

A decomposition (G_D, G_S) of $\tilde{\Gamma}$ is denoted as $\tilde{\Gamma} = G_D \cup G_S$.

In other words, a decomposition of an undirected multigraph is a splitting of its edges into two simple graphs. Of course, an undirected multigraph often admits more than one decomposition. The subscript "D" has been chosen as G_D will be searched as a distance rigid graph. The subscript "S" has been chosen as G_S will be searched as a connected graph in order to synchronize the clocks.

The rank of a distance rigidity matrix is a generic property of its graph [2], let us denote this generic rank simply as $\operatorname{rank} \boldsymbol{R}_D(G)$. Furthermore from (14), the rank of $\boldsymbol{R}_S(G, p)$ is also a generic property of the graph, it is equal to the rank of the incidence matrix of G. Let us denote this generic rank similarly as $\operatorname{rank} \boldsymbol{R}_S(G)$. With these notations, we are now in a position to state our main result.

Theorem 1. *Let (Γ, p) be a generic pseudorange framework whose underlying undirected multigraph is $\tilde{\Gamma}$ and denote $r = \operatorname{rank} \boldsymbol{R}_P(\Gamma, p)$. Then:*

$$r = \max_{\tilde{\Gamma} = G_D \cup G_S} \operatorname{rank} \boldsymbol{R}_D(G_D) + \operatorname{rank} \boldsymbol{R}_S(G_S) \tag{20}$$

where the maximum is taken over the decompositions of $\tilde{\Gamma}$.

Proof. First, consider a decomposition (G_D, G_S) of $\tilde{\Gamma}$ and let us prove that $r \geq \operatorname{rank} \boldsymbol{R}_D(G_D) + \operatorname{rank} \boldsymbol{R}_S(G_S)$. Denote $r_D = \operatorname{rank} \boldsymbol{R}_D(G_D)$ and $r_S = \operatorname{rank} \boldsymbol{R}_S(G_S)$. There exist two square submatrices of $\boldsymbol{R}_D(G_D, p)$ and $\boldsymbol{R}_S(G_S, p)$ of size r_D and r_S with non-null determinants. Let F_D and F_S denote the edge sets associated with their rows, and C_D and C_S the indices of their columns. Then consider $\boldsymbol{N}(\Gamma, p)$ the square submatrix of $\boldsymbol{R}_P(\Gamma, p)$ of size $r_D + r_S$ associated with the columns $C_D \cup C_S$ and the rows $E = F_D \cup F_S$. As in (13), write $\boldsymbol{N}(\Gamma, p) = \begin{bmatrix} \boldsymbol{N}_D(\Gamma, p) & \boldsymbol{N}_S(\Gamma, p) \end{bmatrix}$. By employing the Laplace expansion theorem, see e.g., [14, Section 0.8.9], on the determinant of $\boldsymbol{N}(\Gamma, p)$:

$$\det \boldsymbol{N}(\Gamma) = \sum_{F \subseteq E : |F| = r_S} \pm \det \boldsymbol{N}_D(E \setminus F) \det \boldsymbol{N}_S(F), \tag{21}$$

where the sum is over the subsets of E of cardinality r_S, $\det \boldsymbol{N}(\Gamma)$ denotes the function $p \mapsto \det \boldsymbol{N}(\Gamma, p)$, $\boldsymbol{N}_X(F)$ denotes the submatrix of $\boldsymbol{N}_X(\Gamma)$ induced by the rows of F, and the "$\pm$" depend on the signs of the permutations in the expansion. From (14), the rows of $\boldsymbol{R}_S(F, p)$ are proportional to the columns of the incidence matrix induced by F. Therefore if there is a cycle composed of edges in F and vertices in U, where U denotes the set of vertices associated with the columns C_S, then $\det \boldsymbol{N}_S(F)$ is the null function. Furthermore, if there is no such cycle, $\det \boldsymbol{N}_S(F) = \pm \prod_{uv \in F} D_{u,v}$. Thus, by denoting $\mathcal{F}$ the set of $F \subseteq E$ having cardinality r_S without cycle in U:

$$\det \boldsymbol{N}(\Gamma) = \sum_{F \in \mathcal{F}} P_F \prod_{uv \in F} D_{u,v} \in \mathbb{L}(E). \tag{22}$$

where $P_F = \pm \det \boldsymbol{N}_D(E \setminus F) \in \mathbb{K}$. Equation (22) is the decomposition of $\det \boldsymbol{N}(\Gamma)$ in the natural basis of $\mathbb{L}(E)$. Since $\det \boldsymbol{N}_D(E \setminus F_S, p) = \det \boldsymbol{N}_D(F_D, p) \neq 0$, the coefficient associated with F_S is not null and $\det \boldsymbol{N}(\Gamma) \neq 0$. Therefore, as p is generic according to Lemma 4, $\det \boldsymbol{N}(\Gamma, p) \neq 0$ and $r \geq r_D + r_S$. Thus:

$$r \geq \max_{G_D \cup G_S = \tilde{\Gamma}} \operatorname{rank} \boldsymbol{R}_D(G_D) + \operatorname{rank} \boldsymbol{R}_S(G_S).$$

Conversely, consider a submatrix $\boldsymbol{N}(\Gamma, p)$ of $\boldsymbol{R}_P(\Gamma, p)$ of size r with a non-null determinant. Denote as F its rows. Write similarly $\boldsymbol{N}(\Gamma, p) = \begin{bmatrix} \boldsymbol{N}_D(\Gamma, p) & \boldsymbol{N}_S(\Gamma, p) \end{bmatrix}$. With the same notations as in (21), since $\det \boldsymbol{N}(\Gamma) \neq 0$, there exists $F_S \subseteq F$ such that $\boldsymbol{N}_D(F \setminus F_S) \neq 0$ and $\det \boldsymbol{N}_S(F_S) \neq 0$. Let $F_D = F \setminus F_S$, $r_D = |F_D|$ and $r_S = |F_S|$. Finally, set $E_S = F_S \cup E_2$ and $E_D = E_2 \cup (E_1 \setminus F_S)$ where E_1 and E_2 denote the edge sets of the single and double edges of $\tilde{\Gamma}$. We can verify that $G_D = (V, E_D)$ and $G_S = (V, E_S)$ form a decomposition of $\tilde{\Gamma}$. Furthermore, by construction, $\operatorname{rank} \boldsymbol{R}_D(G_D) \geq r_D$ and $\operatorname{rank} \boldsymbol{R}_S(G_S) \geq r_S$. Thus:

$$\operatorname{rank} \boldsymbol{R}_D(G_D) + \operatorname{rank} \boldsymbol{R}_S(G_S) \geq r_D + r_S = r,$$

concluding the proof of Theorem 1.

□

Theorem 1 implies that two generic pseudorange frameworks having the same underlying undirected graph have rigidity matrices of the same rank. Consequently, from the definition of infinitesimal rigidity, Theorem 1 has the following corollary.

Corollary 1. *Let $\tilde{\Gamma}$ be an undirected pseudorange graph. Either every generic d-dimensional pseudorange framework whose underlying undirected pseudorange graph is $\tilde{\Gamma}$ is rigid or none of them is. In this former case, $\tilde{\Gamma}$ is said to be rigid in $\mathbb{R}^d$.*

This corollary is illustrated by the pseudorange frameworks of Figure 2. The frameworks (Γ_1, p_1) and (Γ_2, p_2) have the same underlying undirected graph, their graphs are both flexible. Note that however the admissible deformations are different. Similarly, the frameworks (Γ_3, p_3) and (Γ_4, p_4) have the same graph and are both rigid.

The second main consequence of Theorem 1 is the characterization of the rigidity of the underlying undirected graph.

Corollary 2. *Let $\tilde{\Gamma}$ be an undirected pseudorange graph. $\tilde{\Gamma}$ is rigid in $\mathbb{R}^d$ if and only if there exists a decomposition (G_D, G_S) of $\tilde{\Gamma}$ such that G_D is distance rigid in $\mathbb{R}^d$ and G_S is connected.*

Proof. Let (Γ, p) be a generic pseudorange framework having $\tilde{\Gamma}$ for underlying undirected pseudorange graph. $\tilde{\Gamma}$ is rigid in $\mathbb{R}^d$ if and only if $\operatorname{rank} \boldsymbol{R}_P(\Gamma, p) = S_P(n, d)$. For any graph G_D, $\operatorname{rank} \boldsymbol{R}_D(G_D) \leq S_D(n, d)$ with equality if and

only if G_D is distance rigid in $\mathbb{R}^d$. Similarly, for any graph G_S, $\operatorname{rank} \boldsymbol{R}_S(G_S) = \operatorname{rank} \boldsymbol{B}(G_S) \leq n-1$ with equality if and only if G_S is connected. As by definition $S_P(n,d) = S_D(n,d) + n - 1$, according to Theorem 1, $\operatorname{rank} \boldsymbol{R}_P(\Gamma, p) = S_P(n,d)$ if and only if there exists a decomposition (G_D, G_S) that achieves both equalities. □

Corollary 2 gives an interpretation to the rigidity of pseudorange frameworks. To be rigid a pseudorange graph should have a decomposition into a distance rigid graph and a connected graph. The distance rigid graph sets the positions of the agents while the connected graph synchronizes their clocks. This decomposition may be viewed as a decoupling of the space and clock variables.

From a combinatorial point of view, Theorem 1 can be stated using *matroid* theory, see e.g., [22]. The pseudorange rigidity matroid is defined on the edges of the directed graph Γ. Its independent sets are the sets of edges that generate independent rows in generic rigidity matrices. Theorem 1 states that the pseudorange rigidity matroid is the union of the distance rigidity matroid with the cycle matroid.

Testing pseudorange rigidity requires testing distance rigidity. In 2D, there exist efficient algorithms, i.e., that run in polynomial time, to verify the rigidity of graphs, see e.g., [16]. However, the distance rigidity matroid is not characterized in 3D and no deterministic algorithm can be employed. In [11], the authors proposed an efficient alternative by employing randomized rigidity tests. The idea is to infer infinitesimal rigidity by computing the rank of a randomly generated configuration with (large) integer coordinates. This test will never return a false positive and the probability to return a false negative is bounded. By repeating the test several times, the probability of error can be reduced to an acceptable level.

An extension of this work could focus on the global rigidity of pseudorange frameworks. As distance rigidity, global distance rigidity is a generic property of the graphs [8], [11]. Global pseudorange rigidity is a generic property neither of the underlying undirected graph nor of the directed graph. Indeed, the two rigid frameworks in Figures 2c and 2d form a counterexample: they have the same graph but one is globally rigid and the other is not. This example is an adaptation of the single-receiver single-constellation problem with 4 satellites and was highlighted in [1] (and [26] for the LORAN system). Future work will study global pseudorange rigidity. In particular, we can adapt Corollary 2 to make the following conjecture.

Conjecture 1. *Let (Γ, p) be a generic pseudorange framework whose underlying undirected pseudorange graph is $\tilde{\Gamma}$. If there exists a decomposition (G_D, G_S) of $\tilde{\Gamma}$ such that G_D is globally rigid in $\mathbb{R}^d$ and G_S is connected, then (Γ, p) is globally rigid.*

This conjecture is motivated by the algebraic methods proposed to solve the usual GNSS positioning problem [4], [18]. When employed with 4 satellites, they provide two candidate solutions. One of these candidates may imply a nonsense, e.g., a negative distance, and should be ruled out. We conjecture that the uniqueness of theses weak solutions is a generic property of the graph and that if we weaken the pseudorange constraint to:

$$\rho_{u,v} = \pm \|x'_u - x'_v\| + \beta'_v - \beta'_u, \tag{23}$$

then global rigidity becomes a generic property of the underlying undirected graph. Future work will focus on proving this conjecture.

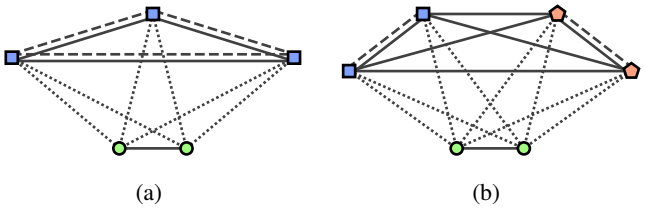

(a) (b)

Fig. 3: GNSS graphs associated with the graphs of measurements of Fig. 1. The edge sets are represented by: dotted lines for E_P, solid lines for E_D, and dashed lines for E_S.

V. GNSS RIGIDITY FOR COOPERATIVE POSITIONING

A. GNSS rigidity

This section presents the adaptation of pseudorange rigidity for cooperative GNSS.

Consider a group of S satellites belonging to C different GNSS constellations and R cooperative receivers. It is assumed that the receivers cooperate by measuring distances. It is also assumed that the positions of the satellites are known and that the satellites belonging to the same constellation are synchronized. We focus on the rigidity of the framework formed by the receivers and the satellites. Each agent (satellite or receiver) is parameterized by $p_i = \begin{pmatrix} x_i^\intercal & \beta_i \end{pmatrix}^\intercal \in \mathbb{R}^{d+1}$. This framework has 3 types of constraints:

1) Pseudorange constraints: from satellites to receivers. They are represented by a directed graph $\Gamma = (V, E_P)$.
2) Distance constraints: between receivers and between satellites. The distance constraints between receivers are due to the distance measurements, while the distance constraints between satellites are due to the fact that their positions are known. As the positions of the satellites are known, so are their inter-distances. Distance constraints are represented by an undirected graph $G_D = (V, E_D)$.
3) Synchronization constraints: between satellites. The satellites within a GNSS constellation are synchronized, therefore if two satellites u and v belong to the same GNSS constellation, then $\beta_u = \beta_v$. These constraints are represented in an undirected graph $G_S = (V, E_S)$.

These three graphs of constraints are grouped into one graph that we call a GNSS graph $\mathcal{G} = (\Gamma, G_D, G_S)$. Similarly to pseudorange graphs, we denote as $\tilde{\mathcal{G}} = (\tilde{\Gamma}, G_D, G_S)$ the underlying undirected GNSS graph. Figure 3 presents the two GNSS graphs associated with the simple cooperative networks introduced in Figure 1. We define a GNSS framework as $(\mathcal{G}, p)$, the combination of the GNSS graph and the pseudorange configuration of the agents. The rigidity matrix of a GNSS framework is:

$$\boldsymbol{R}_G(\mathcal{G}, p) = \begin{bmatrix} \boldsymbol{R}_D(\Gamma, p) & \boldsymbol{R}_S(\Gamma, p) \\ \boldsymbol{R}_D(G_D, p) & \boldsymbol{0} \\ \boldsymbol{0} & \boldsymbol{R}_S(G_S, p) \end{bmatrix}, \tag{24}$$

where the edges of G_S have been oriented.

The theorems for pseudorange frameworks naturally adapt to GNSS frameworks by adapting the decomposition.

Definition 4. *Consider $\tilde{\mathcal{G}} = (\tilde{\Gamma}, G_D, G_S)$ an underlying undirected GNSS graph. Two simple graphs $G'_D = (V, E'_D)$ and $G'_S = (V, E'_S)$ are said to form a* decomposition *of $\tilde{\mathcal{G}}$ if there exists a decomposition $G_{PD} = (V, E_{PD})$, $G_{PS} = (V, E_{PS})$ of $\tilde{\Gamma}$ such that:*

1) $E'_D = E_D \cup E_{PD}$.
2) $E'_S = E_S \cup E_{PS}$.

In other words, the pseudoranges of Γ are divided between the graph of distance constraints and the graph of synchronizations.

Adapting Theorem 1, the rigidity of a GNSS framework is generic property of its underlying undirected graph and Corollary 2 becomes:

Theorem 2. *Let $\tilde{\mathcal{G}}$ be an undirected GNSS graph. $\tilde{\mathcal{G}}$ is rigid in $\mathbb{R}^d$ if and only if there exists a decomposition (G'_D, G'_S) of $\tilde{\mathcal{G}}$ such that G'_D is distance rigid in $\mathbb{R}^d$ and G'_S is connected.*

Proof. As for pseudorange frameworks, the maximal rank of a GNSS rigidity matrix is $S_P(n, d)$. A distance edge $uv \in G_D$ can only increase the rank of the distance part $\boldsymbol{R}_D$. A synchronization edge $uv \in G_S$ can only increase the rank of the bias part $\boldsymbol{R}_S$. Similar to the proof of Corollary 2, the rigidity matrix has maximal rank if and only if there exists a decomposition (G'_D, G'_S) with G'_D and G'_S both having maximal rank, i.e., if and only if there exists a decomposition (G'_D, G'_S) of $\tilde{\mathcal{G}}$ such that G'_D is distance rigid in $\mathbb{R}^d$ and G'_S is connected. □

This result provides a new interpretation for the solvability of GNSS problems.

B. Solvability of GNSS problems

In a GNSS problem, the objective is to find the positions and the clock offsets of the receivers (with respect to some constellation time taken as a reference). A problem is said to be solvable if the measurements allow to isolate solutions, i.e., if the solution set is discrete. Under the natural assumptions that (i) the agents are in a generic configuration, and (ii) the number of satellites is $S \geq d$, the solvability of a GNSS problem is equivalent to the rigidity of the associated GNSS graph. If a GNSS framework is flexible, the measurements are insufficient to identify a specific configuration because of the admissible deformations. On the contrary, if the framework is rigid, there is locally only one configuration realizing the measurements, see [3] for a detailed analysis on the connections between solvability and rigidity (for distance rigidity).

GNSS rigidity provides a new understanding on the minimal number of measures required to locate a GNSS receiver. If a receiver is measuring signals from satellites belonging to C different GNSS constellations, $C + d$ satellites are required to locate it. In this case, C pseudorange measurements are used to connect G'_S, i.e., to synchronize the agents, while the other d rigidify the position of the receiver in G'_D. Consider now the networks illustrated in Figure 3a and 3b. In both figures, each receiver receives signals from only $2 + C$ satellites. Without cooperation, they cannot be located (in 3D) as it would require that they receive signals from at least $C + 3$ satellites. If $C = 1$, the cooperation does not allow the agents to be located. Figure 4 proposes a decomposition of the GNSS graph with the graph G'_S connected. The resulting graph G'_D is not distance rigid in $\mathbb{R}^3$: the agents are connected to only two satellites and can "swing" around them. In the bi-constellation scenario of Figure 3b, the problem of the localization of the agents becomes solvable: Figure 4 presents a decomposition satisfying the condition of Theorem 2.

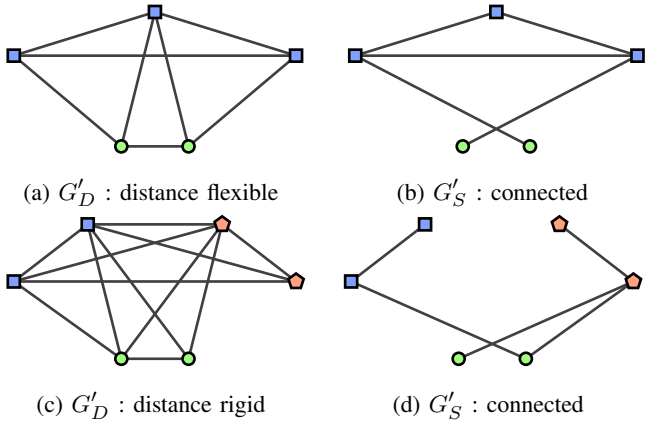

(a) G'_D : distance flexible (b) G'_S : connected

(c) G'_D : distance rigid (d) G'_S : connected

Fig. 4: Decompositions of the GNSS graphs of Fig. 3. Figs. 4a and 4b: Non-rigid decomposition of the GNSS graph of Figure 3a (G'_D is not distance rigid in $\mathbb{R}^3$). Figs. 4c and 4d: rigid decomposition of the GNSS graph of Fig 3b.

Theorem 2 also gives the minimal number of measurements required to locate a network.

Lemma 5. *The minimum number of pseudorange or distance measurements to locate a network of R receivers using satellites from C different constellations is $R(d + 1) + C$.*

Proof. To be locatable, the GNSS graph formed by the receivers and the satellites must be rigid. Therefore, it must have at least $S_P(R+S, d)$ constraints. The proof can be performed by induction. $d+1$ constraints are used to rigidify each receiver and C to synchronize the constellations. □

C. About the estimation of the positions

Estimating the positions of the agents in a network is a difficult question. It has been the subject of numerous studies when only distance measurements are considered, see e.g., [3] or [23]. This paragraph highlights how GNSS rigidity can be used to design estimation algorithms. The algorithm proposed here is for illustrative purposes only. It is based on a perfect setting (no noise or bias), and its robustness and performance should obviously be the subject of specific studies.

The rigidity of the GNSS graph guarantees that the rigidity matrix has a maximum rank. Nevertheless, this matrix has not full rank because of the trivial motions. The rotation and the translation ambiguities are eliminated thanks to the satellites that have known positions. The clock bias ambiguity is removed by taking the first constellation as a reference. If

we decompose the configuration as $p = \begin{pmatrix} p_a^\intercal & p_u^\intercal \end{pmatrix}^\intercal$, where p_a groups all the known parameters (positions of the satellites, and biases of the first constellation), and p_u groups all the unknown parameters, then the columns of $\boldsymbol{R}_G(\Gamma, p)$ associated with p_u have full rank. From (12), the rigidity matrix is proportional to the Jacobian of the measurement function F_G. The rigidity of the GNSS graph implies that the Jacobian of F_G with respect to p_u has full column rank and can be inverted. This property is crucial for the design of estimation algorithms.

For example, it allows to apply Newton's method. This method is already commonly used in the PVT algorithm to estimate the position of a single receiver [17, Section 2.5]. Starting from an initial configuration $p^0 = \begin{pmatrix} p_a^\intercal & p_u^{0\intercal} \end{pmatrix}^\intercal$, the vectors p_u and p are updated until convergence as:

$$p_u^{k+1} \leftarrow p_u^k - \left[\frac{\partial F_G(\Gamma, p^k)}{\partial p_u^k}\right]^+ (F_G(p^k) - y_m), \tag{25a}$$

$$p^{k+1} \leftarrow \begin{pmatrix} p_a^\intercal & p_u^{k+1\intercal} \end{pmatrix}^\intercal, \tag{25b}$$

where $[\cdot]^+$ denotes the pseudo-inverse and y_m is the vector of measurements. If correctly initialized, the algorithm converges to the positions. Once again, this algorithm is just for illustrative purposes and should be further studied in future work. The important point here is that rigidity ensures that the pseudo-inverse can be formed which is essential for the algorithm.

VI. Pseudorange rigidity for formation control

Beyond GNSS, pseudorange rigidity has applications in other fields such as flight formation control. To make a group of UAVs flies in formation, a common strategy is to constrain some of the distances between the UAVs, see e.g., [21]. To maintain the formation, the structure formed by the agents must be rigid. Consequently, it requires at least $S_D(n, d)$ distance measurements. In practice, a distance measurement between UAVs is often carried out using the time-of-flight of a signal between the agents [23]. As in GNSS, since the agents are not synchronized, the time-of-flight does not provided directly the distance between the agents.

If the clocks are modeled simply with a bias, as in (1), the time-of-flight gives the pseudorange between the agents. To suppress the bias, one can apply a symmetrical two-way ranging procedure by making two symmetrical pseudorange measurements and average them: $\delta_{u,v} = (\rho_{u,v} + \rho_{v,u})/2$. Therefore, maintaining the formation with this procedure requires constraining $2S_D(n, d)$ pseudoranges. If the agents were considered as a pseudorange framework instead of as a distance framework, it would require only $S_P(n, d)$ pseudorange constraints to maintain the formation. For large networks, as $2S_D(n, d) \sim_n 2nd$ and $S_P(n, d) \sim_n n(d+1)$, this second procedure reduces the number of measurements by up to 25% in 2D and 33% in 3D.

From an implementation point of view, pseudoranges have another interest. To control a formation the agents may be commanded to maintain only some of the constraints. Formation persistence [13] studies the (distance) rigidity of graphs assuming that the constraints are maintained by only one agent, called the *follower*. If the graph has some properties, the whole formation is preserved. This technique greatly simplifies the command. With the symmetrical two-way ranging procedure, an agent having several followers has to interact with every one of them to compute the distances. When the number of followers increases, the update rate necessarily decreases, which may induce a loss of precision. With the pseudorange approach in contrast, an agent having several followers may not interact with them: he could simply broadcast its position and bias, then, each follower could compute the pseudorange without any feedback. This approach allows significant scale up in the system as the number of followers would not be limited by the channel capacity. Persistence can be adapted to pseudoranges. Consider for example the rigid pseudorange graph in Figure 5. It requires feedback only between the first three agents. The rest of the agents can maintain the formation by maintaining only the pseudorange constraints pointing to them.

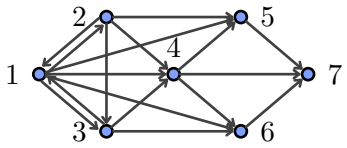

Fig. 5: Example of a rigid formation in $\mathbb{R}^2$.

If the clocks are modeled with a bias and a skew as in (4), the times-of-flight induce the constraints of JPC rigidity. In that situation, the pseudorange becomes:

$$\begin{aligned} \rho_{uv} &\triangleq c\left(t^v_{r(uv)} - t^u_{e(uv)}\right), \\ &= w_v c t_{r(uv)} + \beta_v - w_u c t_{e(uv)} - \beta_u, \\ &= w_v \|x_u - x_v\| + (w_v - w_u) c t_{e(uv)} + \beta_v - \beta_u, \end{aligned}$$

where $\beta_u \triangleq c\tau_u$. In [29], it is assumed that (i) the communication is bi-directional [29, Assumption 1], and (ii) the agents send only one signal at a time $t_{e(u)}$ [29, Assumption 2b], i.e., for all v, $t_{e(uv)} = t_{e(u)}$. In JPC rigidity, an edge constrains both the pseudoranges ρ_{uv} and ρ_{vu}. We can imagine asymmetrical network in which, e.g., some agents are only listening. The resulting framework would have a directed graph as a pseudorange graph. A natural question is: Is asymmetrical JPC rigidity a generic property of the underlying undirected graph? The answer is no. For example, consider a fully connected graph of 4 agents, such a graph is clearly symmetrical. Furthermore, according to [29], it is JPC rigid in $\mathbb{R}^2$. Add a 5th agent, we claim that if we add the arcs $(i, 5)$ for $i = 1, \ldots, 4$, the graph is rigid, while if we add the arcs $(5, i)$ for $i = 1, \ldots, 4$, it is not. Those two graphs are illustrated in Figure 6. Indeed, the constraint induced by the arc $(i, 5)$ is:

$$w_5\left(\|x_i - x_5\| + t_{e(i)}\right) + \beta_i = \rho_{i5} + w_i t_{e(i)} + \beta_i, \tag{26a}$$

while the constraint induced by the arc $(5, i)$ is:

$$w_5 t_{e(5)} + \beta_5 = -\rho_{5i} + w_i(\|x_i - x_5\| + t_{e(5)}) + \beta_i. \tag{26b}$$

Constraint (26a) is similar to a GNSS constraint: with the first four agents set, the RHS is a constant. Generically, with $d+2$

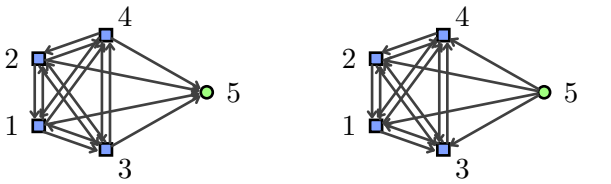

(a) JPC rigid framework. (b) JPC flexible framework.

Fig. 6: Examples of asymmetrical JPC frameworks.

equations the parameters of the 5th agent are set, thus this graph is rigid. On the other hand, from (26b), neither w_5 nor β_5 can be identified but only the sum $w_5 ct_{e(5)} + \beta_5$, thus this graph is flexible. Asymmetrical JPC rigidity is therefore not a generic property of the underlying undirected graph. It is a more complex rigidity, since it uses a more complex clock model, and should be studied in future work.

VII. Conclusion

This paper has introduced a new rigidity based on pseudoranges. It specificity is that the graph of constraints is directed. A complete characterization of generic rigidity of pseudorange graphs is provided based on distance rigidity. A pseudorange rigid graph is the combination of a distance rigid graph and a connected graph. Pseudorange rigidity has been adapted to answer the solvability of GNSS cooperative positioning problems. It was also highlighted how rigidity can be used to design algorithms to solve the positioning problem. Finally, the interest of pseudorange rigidity has been presented in formation control with a comparison with the recently introduced Joint Position-Clock rigidity.

Three possible future research directions have been suggested. The first is the study of global pseudorange rigidity. Once adapted to GNSS, it can provide the condition for the uniqueness of the solution. The second is the derivation of specific algorithms to estimate the positions of the agents. The third is the adaptation of pseudorange rigidity with more complex clock models.

Appendix I
Proof of Lemma 3

Lemma 3 is the application of the following lemma.

Lemma 6. *Let $\mathbb{K} = \mathbb{Q}(X_1, \dots, X_N)$ be the field of fractions in N variables with coefficients in $\mathbb{Q}$ and $(R_1, \dots, R_m)$ be a family of functions such that:*

H.1 $\forall i \in \{1, \dots, m\}$, $R_i^2 \in \mathbb{K}$;

H.2 $\forall i \in \{1, \dots, m\}$, $R_i^2 \notin \mathbb{K}^{(2)}$, *with* $\mathbb{K}^{(2)} = \{P^2 \mid P \in \mathbb{K}\}$;

H.3 $\forall I \in \boldsymbol{\mathcal{P}}(\{1, \dots, m\}) \setminus \{\emptyset\}$, $R_I = \prod_{i \in I} R_i \notin \mathbb{K}$.

Then $\mathbb{L} = \mathbb{K}[R_1, \dots, R_m]$ is a field and $\mathbb{L}/\mathbb{K}$ is a field extension of order 2^m.

Proof. The proof is realized by induction over m. The property to prove is $\mathbf{P}(k)$: "For any $R_1, \dots, R_k$ satisfying the three hypotheses, $\mathbb{L} = \mathbb{K}[R_1, \dots, R_k]$ is a field and $\mathbb{L}/\mathbb{K}$ is a field extension of order 2^k."

Initialization. For $k = 1$, let R satisfy the three hypotheses. To prove that $\mathbb{K}[R]$ is a field, proving that every non-null element has an inverse is sufficient. Let $P \in \mathbb{K}[R]$, $P \neq 0$. Since $R^2 \in \mathbb{K}$, there exists $(A, B) \in \mathbb{K}^2$ with $(A, B) \neq (0, 0)$ such that $P = A + BR$. If $B = 0$, $P = A \in \mathbb{K}$ therefore P is invertible. If $B \neq 0$, using Hypothesis H.2, $R^2 \neq A^2/B^2$, therefore $A^2 - B^2R^2 \neq 0$. Then, $(A - BR)/(A^2 - B^2R^2) \in \mathbb{K}[R]$ is the inverse of P. The extension is of order 2 by Hypothesis H.1 and Hypothesis H.3. Thus, $\mathbf{P}(1)$ is true.

Induction step. Assume $\mathbf{P}(k)$ for $k \geq 1$ and prove $\mathbf{P}(k+1)$. Let $R_1, \dots, R_{k+1}$ be $k+1$ functions satisfying the three hypotheses. We denote $\mathbb{L}_k = \mathbb{K}[R_1, \dots, R_k]$. First, let us prove that $\mathbb{L}_{k+1}$ is a field. Proving that $R_{k+1}^2 \notin \mathbb{L}_k^{(2)}$ is sufficient since then, with the same arguments as for the initialization every non-null element of $\mathbb{L}_{k+1}$ would have an inverse.

Let us assume by contradiction that $R_{k+1}^2 \in \mathbb{L}_k^{(2)}$. By induction hypothesis, $\mathbb{L}_k = \mathbb{L}_{k-1}[R_k]$. Therefore, there exist $A, B \in \mathbb{L}_{k-1}$ such that:

$$R_{k+1}^2 = (A + BR_k)^2 = A^2 + B^2R_k^2 + 2ABR_k \qquad (27)$$

If $AB \neq 0$, then $R_k \in \mathbb{L}_{k-1}$ which contradicts the induction hypothesis. Then, necessarily A or B is null. If $B = 0$, then $R_{k+1}^2 = A^2 \in \mathbb{L}_{k-1}^{(2)}$ This also contradicts the induction hypothesis when considering the k functions $R_1, \dots, R_{k-1}, R_{k+1}$. Therefore $A = 0$. If $A = 0$ then, $R_{k+1}^2 = B^2R_k^2$ and $(R_{k+1}R_k)^2 = (BR_k^2)^2 \in \mathbb{L}_{k-1}^{(2)}$. Similarly, this also contradicts the induction hypothesis when considering the k functions $R_1, \dots, R_{k-1}, R_kR_{k+1}$ (which satisfies the three hypotheses). Theses contradictions give that $R_{k+1}^2 \notin \mathbb{L}_k^{(2)}$ and thus, $\mathbb{L}_{k+1}$ is a field.

To prove the order, let us use the induction hypothesis:

$$[\mathbb{L}_{k+1} : \mathbb{K}] = [\mathbb{L}_{k+1} : \mathbb{L}_k][\mathbb{L}_k : \mathbb{K}] = 2^k[\mathbb{L}_{k+1} : \mathbb{L}_k] \qquad (28)$$

Since $R_{k+1} \notin \mathbb{L}_k$ and $R_{k+1}^2 \in \mathbb{L}_k$, $[\mathbb{L}_{k+1} : \mathbb{L}_k] = 2$ and $[\mathbb{L}_{k+1} : \mathbb{K}] = 2^{k+1}$. $\mathbf{P}(k+1)$ is true. □

Proof of Lemma 3. Let $E \subseteq \{uv \mid 1 \leq u < v \leq N\}$ be a set of edges and $m = |E|$. The set of m distance functions $D_{u,v}$ do satisfy the three conditions of Lemma 6 when $d \geq 2$.

Note however that when $d = 1$, the distance functions do not satisfy Hypothesis H.2 of Lemma 6. □

References

[1] J. S. Abel and J. W. Chaffee. Existence and uniqueness of gps solutions. *IEEE Transactions on Aerospace and Electronic Systems*, 27(6):952–956, 1991.

[2] L. Asimow and B. Roth. The rigidity of graphs. *Transactions of the American Mathematical Society*, 245:279–289, 1978.

[3] J. Aspnes, T. Eren, D. K. Goldenberg, A. S. Morse, W. Whiteley, Yang R. Yang, B. D. O. Anderson, and R. N. Belhumeur. A theory of network localization. *IEEE Transactions on Mobile Computing*, 5(12):1663–1678, 2006.

[4] S. Bancroft. An algebraic solution of the gps equations. *IEEE transactions on Aerospace and Electronic Systems*, (1):56–59, 1985.

[5] B. Bollobás. *Modern graph theory*, volume 184. Springer Science & Business Media, 1998.

[6] F. Causa, A. R. Vetrella, G. Fasano, and D. Accardo. Multi-uav formation geometries for cooperative navigation in gnss-challenging environments. In *IEEE/ION position, location and navigation symposium (PLANS)*, pages 775–785, Monterey, CA, USA, 2018.

[7] L. Chen, M. Cao, and C. Li. Angle rigidity and its usage to stabilize multiagent formations in 2-d. *IEEE Transactions on Automatic Control*, 66(8):3667–3681, 2020.

[8] R. Connelly. Generic global rigidity. *Discrete & Computational Geometry*, 33(4):549, 2005.

[9] R. L. Frank. Current developments in Loran-C. *Proceedings of the IEEE*, 71(10):1127–1139, 1983.

[10] H. Gluck. Almost all simply connected closed surfaces are rigid. *Geometric Topology*, pages 225–239, 1975.

[11] S. J. Gortler, A. D. Healy, and D. P. Thurston. Characterizing generic global rigidity. *American Journal of Mathematics*, 132(4):897–939, 2010.

[12] B. Hendrickson. Conditions for unique graph realizations. *SIAM journal on computing*, 21(1):65–84, 1992.

[13] Julien M. Hendrickx, Brian D. O. Anderson, Jean-Charles Delvenne, and Vincent D. Blondel. Directed graphs for the analysis of rigidity and persistence in autonomous agent systems. *International Journal of Robust and Nonlinear Control*, 17(10-11):960–981, 2007.

[14] R. A. Horn and C. R. Johnson. *Matrix analysis*. Cambridge university press, 2012.

[15] B. Jackson. Notes on the rigidity of graphs. In *Levico Conference Notes*, volume 4, 2007. Available at `https://webspace.maths.qmul.ac.uk/b.jackson/levicoFINAL.pdf`.

[16] D. J. Jacobs and B. Hendrickson. An algorithm for two-dimensional rigidity percolation: the pebble game. *Journal of Computational Physics*, 137(2):346–365, 1997.

[17] E. D. Kaplan and C. Hegarty. *Understanding GPS/GNSS: principles and applications*. Artech house, 2017.

[18] L. O. Krause. A direct solution to gps-type navigation equations. *IEEE Transactions on Aerospace and Electronic Systems*, (2):225–232, 1987.

[19] A. Minetto, G. Falco, and F. Dovis. On the trade-off between computational complexity and collaborative gnss hybridization. In *IEEE 90th Vehicular Technology Conference (VTC2019-Fall)*, pages 1–5, Honolulu, HI, USA, 2019.

[20] A. Nixon, B. Schulze, S.-I. Tanigawa, and W. Whiteley. Rigidity of frameworks on expanding spheres. *SIAM Journal on Discrete Mathematics*, 32(4):2591–2611, 2018.

[21] R. Olfati-Saber and R. M. Murray. Graph rigidity and distributed formation stabilization of multi-vehicle systems. In *Proceedings of the 41st IEEE Conference on Decision and Control*, volume 3, pages 2965–2971, Las Vegas, NV, USA, 2002.

[22] James G Oxley. *Matroid theory*, volume 3. Oxford University Press, USA, 2006.

[23] N. Patwari, J. N. Ash, S. Kyperountas, A. O. Hero, R. L. Moses, and N. S. Correal. Locating the nodes: cooperative localization in wireless sensor networks. *IEEE Signal processing magazine*, 22(4):54–69, 2005.

[24] S. Roman. *Field theory*, volume 158. Springer Science & Business Media, 2005.

[25] F. V. Saliola and W. Whiteley. Some notes on the equivalence of first-order rigidity in various geometries. *arXiv preprint arXiv:0709.3354*, 2007.

[26] R. O. Schmidt. A new approach to geometry of range difference location. *IEEE Transactions on Aerospace and Electronic Systems*, (6):821–835, 1972.

[27] B. Schulze, H. Serocold, and L. Theran. Frameworks with coordinated edge motions. *SIAM Journal on Discrete Mathematics*, 36(4):2602–2618, 2022.

[28] B. Schulze and W. Whiteley. Coning, symmetry and spherical frameworks. *Discrete & Computational Geometry*, 48(3):622–657, 2012.

[29] R. Wen, E. Schoof, and A. Chapman. Clock rigidity and joint position-clock estimation in ultra-wideband sensor networks. *IEEE Transactions on Control of Network Systems*, 10(3):1209–1221, 2023.

[30] S. Zhao and D. Zelazo. Bearing rigidity and almost global bearing-only formation stabilization. *IEEE Transactions on Automatic Control*, 61(5):1255–1268, 2015.

[31] S. Zhao and D. Zelazo. Bearing rigidity theory and its applications for control and estimation of network systems: Life beyond distance rigidity. *IEEE Control Systems Magazine*, 39(2):66–83, 2019.

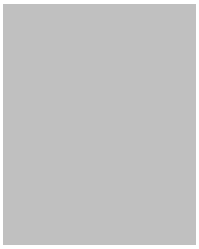

Colin Cros received the Ingénieur degree in Computer Science from École Centrale de Lyon in 2020. He is currently a Ph.D candidate in SIPT (Signal, Image, Speech-Parole, Telecom) at the University of Grenoble, France in collaboration between the GIPSAlab and the company TELESPAZIO France. His areas of research encompass estimation theory and network systems, with a specific focus on applications related to cooperative localization.

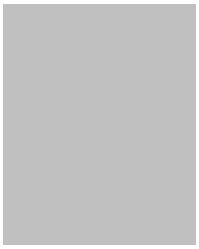

Pierre-Olivier Amblard received the Ingénieur degree in electrical engineering in 1990 from Ecole Nationale Supérieure des Ingénieurs Electriciens de Grenoble, Institut National Polytechnique de Grenoble. He received the DEA (MSc) in signal processing and the Doctorat (PhD) in 1990 and 1994 respectively, both from the INPG. He received the Habilitation à Diriger des Recherches in 2001. Since 1994, he works for the Centre National de la Recherche Scientifique (CNRS) where he is a Directeur de Recherche. He is with GIPSAlab, Grenoble, France, in the GAIA team (Geometry, Learning—Apprentissage, Information and Algorithms). From 2010 to 2013, he was in secondment in the Department of Mathematics and Statistics of the University of Melbourne. His research interests include statistical signal processing, non-stationary signal processing, applications of signal processing in physics.

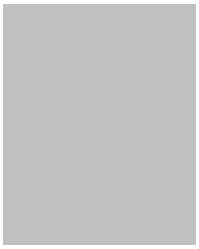

Christophe Prieur is currently a senior researcher of the CNRS at Gipsa-lab, Univ. Grenoble Alpes. He is currently an associate editor of the AIMS Evolution Equations and Control Theory, the SIAM Journal of Control and Optimization and the Mathematics of Control, Signals, and Systems. He is currently an associate editor of the AIMS Evolution Equations and Control Theory, the SIAM Journal of Control and Optimization and the Mathematics of Control, Signals, and Systems. He is a senior editor of the IEEE Control Systems Letters, and an editor of the IMA Journal of Mathematical Control and Information. His current research interests include nonlinear control theory, hybrid systems, and control of partial differential equations, with applications including navigation and object tracking, fluid dynamics, and fusion control. He is an IMA Fellow, and an IEEE Fellow.

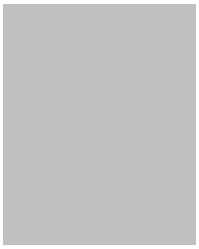

Jean-François Da Rocha is a senior GNSS navigation engineer mainly in Galileo and EGNOS with several years of experience in Avionics and Spacecraft embedded systems, and Mission and Control Centre (LEO Constellation) including management level. He participated to the PPP with integer ambiguity resolution for GPS and Galileo using satellite products from different analysis centers. He is currently working on Galileo Public Regulated Service Initial and Full Operational Capability.